Proline- and Arginine-Rich Peptides Constitute a Novel Class of Allosteric Inhibitors of Proteasome Activity †

ARTICLE *in* BIOCHEMISTRY · AUGUST 2003

Impact Factor: 3.02 · DOI: 10.1021/bi034784f · Source: PubMed

5 AUTHORS, INCLUDING:

Maria Gaczynska
University of Texas Health Science Center at …
85 PUBLICATIONS **2,971** CITATIONS
SEE PROFILE

Pawel A Osmulski
University of Texas Health Science Center at …
47 PUBLICATIONS **825** CITATIONS
SEE PROFILE

Youhe Gao
Beijing Normal University
76 PUBLICATIONS **1,499** CITATIONS
SEE PROFILE

Accelerated Publications

Proline- and Arginine-Rich Peptides Constitute a Novel Class of Allosteric Inhibitors of Proteasome Activity†

Maria Gaczynska,*,‡ Pawel A. Osmulski,‡ Youhe Gao,§ Mark J. Post,|| and Michael Simons||

Institute of Biotechnology, University of Texas Health Science Center at San Antonio, 15355 Lambda Drive, San Antonio, Texas 78245, Institute of Basic Medical Science, Peking Union Medical College, Beijing, China, and Angiogenesis Research Center and Section of Cardiology, Departments of Medicine, Dartmouth-Hitchcock Medical Center, Dartmouth Medical School, Lebanon, New Hampshire 03755

Received May 14, 2003; Revised Manuscript Received June 18, 2003

ABSTRACT: Substrate-specific inhibition of the proteasome has been unachievable despite great interest in proteasome inhibitors as drugs. Recent studies demonstrated that PR39, a natural proline- and arginine-rich antibacterial peptide, stimulates angiogenesis and inhibits inflammatory responses by specifically blocking degradation of IκBα and HIF-1α by the proteasome. However, molecular events involved in the PR39−proteasome interaction have not been elucidated. Here we show that PR39 is a noncompetitive and reversible inhibitor of the proteasome function. This effect is achieved by a unique allosteric mechanism allowing for specific inhibition of degradation of selected proteins without affecting total proteasome-dependent proteolysis. Atomic force microscopy (AFM) studies demonstrate that 20S and 26S proteasomes treated with PR39 or its derivatives exhibit serious perturbations in their structure and their normal allosteric movements. These effects are universal for proteasomes from yeast to human. The shortest functional sequence derived from PR39 still showing the allosteric inhibitory effect consists of eleven NH_2-terminal residues containing essential three NH_2-terminal arginines. The noncompetitive and reversible in vitro action of PR39 and its truncated derivatives is matched by the ability of the peptides to induce angiogenesis in vivo. We postulate that PR39 changes conformational dynamics of the proteasomes by interactions with the noncatalytic subunit α7 in a way that prevents the enzyme from cleaving the substrates of unique structural constraints.

Recent studies demonstrated that PR39,[1] a proline/arginine-rich 39-amino-acid peptide originally derived from porcine bone marrow, exhibits a broad spectrum of biological activities, including the ability to induce angiogenesis (*1*) and to limit inflammatory damage in a variety of animal models (*2*−*5*). The angiogenic effect of the peptide is in part explained by its ability to inhibit proteasome-dependent degradation of the transcription factor HIF-1α, while anti-inflammatory activity is associated with inhibition of IκBα degradation that in turn prevents activation of NFκB-dependent gene expression (*6*). Furthermore, in yeast two-hybrid screens, the peptide has been shown to bind to the α7 subunit of the 20S proteasome (*6*). However, no direct link has been established among the peptide binding to a noncatalytic proteasome subunit, inhibition of proteasome proteolytic activity, and biological activity of the peptide. The present investigation was undertaken to address this issue.

The proteasome, or multicatalytic proteinase, is responsible for the majority of nonlysosomal proteolysis in eukaryotic cells (*7*). The enzyme is a giant assembly of multiple subunits, with diverse activities and a modular structure. Its 28 subunits of the 20S catalytic core are arranged into four stacked rings, each containing seven subunits. The outer α rings contain only noncatalytic α subunits, whereas each of the two inner β rings harbor three active centers concealed inside the barrel-like structure with NH_2-terminal threonines as catalytic residues. The three active centers have distinct specificities named chymotrypsin-like (ChT-L), trypsin-like (T-L), and peptidylglutamyl peptide hydrolyzing (PGPH or caspase-like) activities. They cleave polypeptides on the COOH-terminal sides of hydrophobic, basic, or acidic amino

† The work was supported by the R01 HL70247 Grant (M.S.).

* Corresponding author. Tel: (210) 567-7262. Fax: (210) 567-7269. E-mail: gaczynska@uthscsa.edu.

‡ University of Texas Health Science Center at San Antonio.

§ Peking Union Medical College.

|| Dartmouth Medical School

[1] Abbreviations: AcYVAD-MCA, *N*-acetyl-TyrValAlaAsp-MCA; AFM, atomic force microscopy; BocLRR-MCA, N-*tert*-butoxycarbonyl-LeuArgArg-MCA; Cbz-LLE-MCA, N-carboxybenzyl-LeuLeuGlu-MCA; ChT-L, chymotrypsin-like; DMSO, dimethyl sulfoxide; HIF-1α, hypoxia inducible factor 1α; IκBα, inhibitory subunit of NFκB (nuclear factor κ B); MCA, 7-amino-4-methylcoumarin; MWC, molecular weight cutoff; PGPH, peptidylglutamyl peptide hydrolyzing; PR39, proline- and arginine-rich 39-amino-acid-long (peptide); SDS, sodium dodecyl sulfate; SucAAF-MCA, SucAlaAlaPhe-MCA; SucLLVY-MCA, N-succinyl-LeuLeuValTyr-MCA; TFA, trifluoroacetic acid; T-L, trypsin-like.

10.1021/bi034784f CCC: $25.00
Published on Web 07/04/2003

acid residues, respectively. The 20S proteasome alone is able to degrade small peptides and unfolded proteins. The 20S particle with attached two 19S complexes forms 26S (2500 kDa) proteasome responsible for recognition and degradation of proteins tagged with polyubiquitin chains (*7*, *8*).

Since the proteasome cleaves numerous cell cycle regulators, antigenic proteins, and transcription factors, it is an attractive target for the development of drugs for the treatment of cancer, autoimmune diseases, muscle wasting, and inflammation, among other pathological states. Currently, a peptidyl boronate and a lactone derivative, competitive inhibitors of proteasome activity, are in clinical trials involving multiple cancers and stroke, respectively. These compounds, as all other currently known proteasomal inhibitors, block active centers of the enzyme, indiscriminately halting cleavage of all proteasomal substrates in the cell, triggering apoptosis (*9*−*11*).

In contrast to the competitive inhibitors, allosteric inhibitors offer a potential for more precise, substrate-specific regulation of proteasome activity. Until now, however, no compound has been shown to exhibit such interactions with the proteasome. In this study, we demonstrate that PR39 peptide, previously shown to selectively affect proteasome-mediated protein degradation in vivo, alters the shape of the 20S cylinder and affects the binding of 19S caps in a reversible manner. The ability of the peptide and its variants to affect the proteasome shape correlates with the observed biological activities of the peptide. The peptide, therefore, represents a new class of allosteric inhibitors that may form the basis for precise manipulations of proteasome function.

EXPERIMENTAL PROCEDURES

PR Peptides. Synthetic PR peptides were generated following the porcine sequence (RRRPRPPYLPRPRPPPFFP-PRLPPRIPPGFPPRFPPRFP for PR39), purified by HPLC (Genemed Synthesis, Inc.), and dissolved in DMSO.

Source of Proteasome. Proteasomes from the following sources were used: *Homo sapiens*, HeLa.S3 cervical carcinoma cells (American Tissue Type Collection); *Mus musculus*, Sol8 myoblasts (kindly provided by Barbara Christy, UTHSCSA); *Saccharomyces cerevisiae*, strain MHY501 (a kind gift of Mark Hochstrasser, Yale University); *Schizosaccharomyces pombe*, strain 972h$^-$ (a kind gift of Charles Hoffman, Boston College). The 20 and 26S proteasomes were purified as described (*12*, *13*).

Determination of Enzymatic Activity. Peptidase activity was measured with fluorogenic model peptides as the amount of a fluorescent MCA group released after 1 h incubation at 37 °C in 50 mM Tris HCl buffer pH 8.0 containing 0.01% SDS. One hundred μM substrates were used, unless specified otherwise. The following substrates were tested (Bachem AG, Switzerland): ChT-L activity with SucLLVY-MCA and SucAAF-MCA; T-L activity with BocLRR-MCA; PGPH/caspase-like activity with Cbz-LLE-MCA and AcYVAD-MCA. Values of K_M, K_i, and V_{max} were calculated in a range from 5 to 500 μM of substrate concentrations from the Lineweaver−Burk plots following the Michaelis−Menten formalism (*13*). I_{50} (the concentration of a compound causing 50% inhibition) was determined on the basis of inhibitory effect of 0.02−10 μM PR peptides on hydrolysis of 100 μM SucLLVY-MCA. To determine the influence of pH on the inhibitory effect of PR39 (1 μM) and competitive inhibitors, $CbzL_3$-VS (Cbz-LeuLeuLeu-vinyl sulfone, 4 μM) and YU101 (Ac-hPheLeuPheLeu-epoxyketone, 5 nM, both from Calbiochem), the degradation of SucLLVY-MCA by SDS-activated yeast 20S proteasome was monitored in 50 mM Tris/HCl buffers ranging from a pH 7.0 to 8.5. To test the reversibility of proteasome inhibition with PR39, the ChT-L activity with 100 μM SucLLVY-MCA was measured in the following samples: (1) control 10 nM human proteasome (no inhibitor added), pretreated for 10 min with 1% DMSO (the solvent for PR39), and then washed with 500 volumes of 50 mM Tris/HCl buffer, pH 8, on a membrane concentrator (Vivaspin MWC 100,000, Vivascience-Sartorius); (2) proteasomes pretreated for 10 min with 1 μM PR39 and then washed as above; and (3) proteasomes pretreated with PR39 and washed as above, then incubated with 1 μM PR39.

Reverse-Phase HPLC. To determine if the peptides were subjected to proteolytic cleavage catalyzed by the proteasome, we tested products arising from incubation of the peptides with proteasomes by reverse phase chromatography. The reaction mixtures containing either the PR peptides alone (control) or the peptides and human 20S proteasome in 50 mM Tris HCl buffer, pH 8.0, were incubated for up to 5 h. at 37 °C. The mixtures were then separated on an R2M Poros (PerSeptive Biosystems) column. Chromatograms were developed with a linear gradient of acetonitrile from 5−60% in water containing 0.1% TFA.

In Vivo Matrigel Assays. The assay was carried out as described (*1*), using an extract of kidney basement membrane (Matrigel) as a substrate for new blood vessels growth. In brief, 0.5 mL Matrigel (Becton Dickinson) mixed with PR39 peptide or its derivatives (1μg/mL) was injected subcutaneously in the abdominal midline of C57BL/6 mice. Fourteen days later, the pellets were harvested, and thin sections (5 μm) were immunostained with anti-CD31 antibody. Ten random fields of section images at 40X magnification acquired with a high-resolution digital color camera were analyzed using automated image analysis software (Optimas 6.0) to count the number of vessels formed in Matrigel pellets (*1*).

AFM Images. AFM images were collected with Nanoscope IIIa microscope (Digital Instruments), as described (*14*, *15*). The unfixed and unmodified proteasomes in 5 mM Tris-HCl buffer (pH 7.0) were attached to the mica substrate with electrostatic forces, mounted in a wet chamber, and imaged in a tapping mode in liquid, using oxide-sharpened silicon nitride tips with cantilevers of nominal spring constant 0.32 N/m (Nanoprobe; (*14*)). Areas ranging from 0.04 to 1 μm^2 were continuously scanned with a rate of 2.1 Hz, which corresponded to one scan per 4 min. The pixel size (apparent resolution) ranged from 1 to 4 nm. The inhibitors or substrates were injected directly into the wet chamber to the final concentrations of 1−10 μM (inhibitors) or 100 μM (substrate). Typically, 10 μL of 5 mM Tris-HCl buffer mixed with 0.5−1 μL of stock solutions of inhibitors or SucLLVY-MCA dissolved in DMSO was injected. Injection of buffer mixed with DMSO only did not induce detectable differences in the structure and dynamics of 20S proteasomes (*14*). For the inhibitor wash-out experiment, a field of *S. cerevisiae* 20S proteasomes was imaged in control conditions (5 mM Tris/HCl buffer, pH 7, no inhibitor); then PR39 was added to the final concentration of 5 μM and the imaging resumed. After several scans, the inhibitor was removed from the

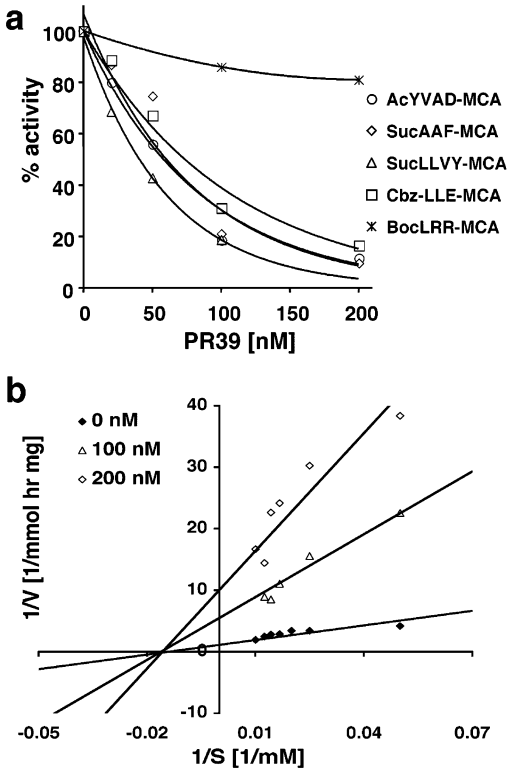

FIGURE 1: PR39 is a noncompetitive inhibitor of human 20S proteasomes in vitro. a, PR39 affects the three major peptidase activities of 20S proteasome to a different degree. ChT-L activity was tested with SucLLVY-MCA and SucAAF-MCA, T-L activity with BocLRR-MCA, and PGPH/caspase-like activity with Cbz-LLE-MCA and AcYVAD-MCA. The substrates were used at 100 μM concentration. b, PR39 noncompetitively inhibits ChT-L activity of human proteasomes as shown with the Lineweaver−Burk plots of the control and PR39-treated proteasomes. Analysis was done with SigmaPlot (SPSS Science) software. The collected data followed the model of noncompetitive inhibition (98% confidence level): calculated maximum velocities, V_{max}, were 0.909, 0.182, and 0.100 μmol of MCA released by 1 mg of the protein during 1 h incubation at 24 °C (for 0, 100, and 200 nM of PR39, respectively), the corresponding Michaelis constant, K_M, was 66 μM, and the K_i value was 25 nM.

sample still mounted in the sample holder by exchange of the buffer (five washes with 500 μL of fresh 5 mM Tris/HCl buffer), and continuous scanning and imaging resumed.

RESULTS AND DISCUSSION

To determine effects of PR39 on the proteolytic activity of proteasomes in vitro, we tested cleavage of a set of fluorogenic peptides representing standard model substrates for the three peptidase activities of SDS-activated 20S proteasomes in the presence of variable concentrations of the peptide. A low concentration of SDS is commonly used to "activate" 20S particles for in vitro studies. The incubation of purified and SDS-activated human 20S proteasomes with PR39 resulted in a dose-dependent inhibition of all the peptidase activities, with the T-L activity being least affected (Figure 1a).

The observed inhibition was not limited to the human 20S proteasome since the peptide was also effective against the particles isolated from *S. cerevisiae*, *S. pombe*, and mouse myoblasts. The peptide was most efficient toward the human 20S proteasome for which the I_{50} was 27±3 nM (n = 5 separate preparations), whereas for *S. cerevisiae* the I_{50} was 0.58 ± 0.12 μM (n = 6 preparations), as determined with 100 μM SucLLVY-MCA. Human 26S proteasome activity was inhibited in vitro by PR39 as well (Figure 2). Therefore, we confirm that PR39 is a strong and universal proteasomal inhibitor.

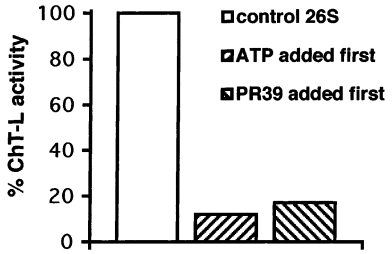

FIGURE 2: PR39 inhibits human 26S proteasomesin vitro. The relative activities are plotted as percents of the velocity of degradation of SucLLVY-MCA by the control proteasomes (100% activity). 26S proteasomes were treated with 1 μM PR39. Additionally, the bars show that the order of addition of agents promoting stability of 26S proteasomes (ATP, Mg^{2+} and DTT (1,4-dithiothreitol)) and PR39 to already assembled 26S proteasomes (ATP or PR39 added first) did not affect the potential of the peptide to inhibit the protease. Averages of two independent experiments are shown. Compare also results shown in Figure 3.

Kinetic analysis of PR39 interactions with 20S proteasomes showed a pattern consistent with a noncompetitive mode of action (Figure 1b). This result suggests that sites of PR39 binding on 20S proteasomes are distinct from the active centers. Furthermore, this is in concert with the outcome of yeast two-hybrid binding assays, which showed that the inhibitor interacts with the noncatalytic subunit α7 (*6*). In addition, the kinetic data imply that PR39 does not preferentially bind to an enzyme−substrate complex. Since incubations of PR39 for as long as several hours in the presence of the protease did not lead to any detectable decrease of amount of the substrate nor formation of any products when tested with RP-HPLC, we concluded that the peptide was not a substrate for 20S proteasomes. This result confirms our observation that the percent of inhibition of the 20S proteasome by PR39 or a truncated variant, PR11, remained unchanged even when degradation of SucLLVY-MCA was continuously monitored for up to 5 h (data not shown).

Moreover, PR39 is probably not trapped by the 20S proteasome, nor does it induce any permanent change in the structure of proteasome since the actions of the peptide were easily reversible. This conclusion is based on results of the following "washing-out" experiments. Human 20S proteasomes were pretreated with 1 μM PR39, and subsequently the inhibitor was washed out with 500 volumes of a reaction buffer. The ChT-L activity of the washed proteasome preparation did not differ from the activity of control (107% of the activity compared to the identically processed control sample not pretreated with the inhibitor). However, readdition of PR39 (1 μM final concentration) to the washed proteasome sample led to severe inhibition of the substrate degradation, with 9% of the activity remaining, as compared with the control.

Since putative PR39 binding to the α7 subunit (*6*) could influence the interaction between 20S and 19S proteasome components, we tested whether PR39 affected assembly of the 26S complexes. For this purpose, 19S and 20S particles were separately purified with a column chromatography and

Order of addition	Reagent added	A	B	C	D
1	20S	+	+	+	+
2	19S	+	-	-	+
3	19S+ATP+DTT+Mg	-	+	+	-
4	PR39	-	-	+	+
5	ATP+DTT+Mg	-	-	-	+
6	SucLLVY-MCA	+	+	+	+

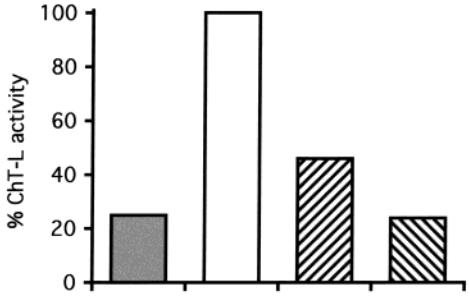

FIGURE 3: PR39 interferes with the assembly of human 26S proteasomes from 20S and 19S particles. The 19S and 20S complexes were purified as individual particles (*12*). Subsequently, they were assembled in the presence of 2mM ATP, 5mM Mg^{2+}, 1 mM DTT, and 1 μM PR39. The bars show that order of addition of the reagents (a chart above the bars) influenced the rate of degradation of the SucLLVY-MCA substrate. The differences in activity can most plausibly be explained by differences in efficiency of the formation of 26S proteasomes. Assembly was hindered if PR39 was added before formation of the complex. Averages of two independent experiments are shown. A, mixture of 20S and 19S complexes; functionally there are only 20S proteasomes since the factors necessary for recreation of 26S particles were absent. B, mixture of 20S and 19S complexes formed functional 26S particles after addition of ATP, DTT and Mg^{2+}. C, 26S proteasomes recreated as in experiment B were treated with 1 μM PR39. D, mixture of 20S and 19S complexes were treated with PR39 before the factors promoting reassembly of 26S proteasomes were added.

native PAGE. Purified complexes were reassembled by addition of 2mM ATP and 5mM Mg^{2+} either in the presence or absence of 1 μM PR39 (Figure 3). A high degree of reassembly (at least 80%) of 26S complexes was deduced from the 4-fold increase in ChT-L peptidase activity after addition of ATP and Mg^{2+} to the mixture. PR39 inhibited the reassembled 26S proteasomes by about 50%. However, when PR39 was added to the mixture before the assembly reaction (before adding ATP and Mg^{2+}), the activity decreased to about 20% of the control sample, suggesting that PR39 interfered with assembly of 26S proteasomes. The 26S particles isolated from human HeLa cells in their native form (not assembled in vitro) were not sensitive to the order of addition of the reagents (Figure 2), since they were always inhibited by PR39 to less than 20% of ChT-L activity of the control proteasomes. At this point it is unclear if the peptide directly competes with the 19S subunits for the same binding site on the α ring, induces structural changes on the α ring that lead to disabling of the binding site, or interferes with the ATPase activity of the 19S base thus inhibiting the process of assembly of 26S complex. The decreased PR39 sensitivity of the in vitro reassembled 26S proteasomes (Figure 3) compared with that of the native 26S complexes (Figure 2) indicates that the inhibitor may also interact with sites on 19S particles buried in the native 26S proteasomes. However, the determination of all the sources of interference was not possible since the in vitro reassembly of proteasomes did not proceed with 100% yield.

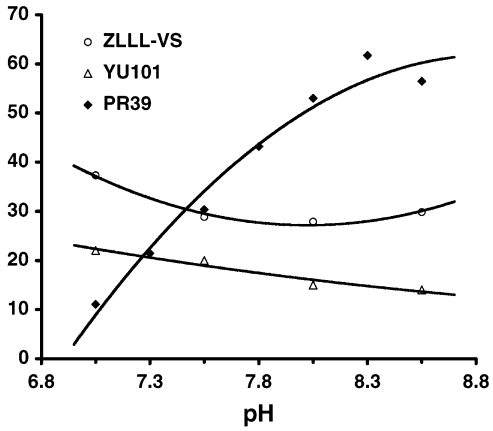

FIGURE 4: The inhibitory effect of PR39 strongly depends onthe charge of interacting residues. Influence of pH on inhibition of *S. cerevisiae* 20S proteasomes by either 1 μM PR39 or competitive inhibitors: 4 μM $CbzL_3$-VS and 5 nM YU101 were tested with SucLLVY-MCA. Within a pH range 7.0−8.5, the efficiency of inhibition by PR39 sharply decreased with the increasing pH. Under the same conditions, the inhibitory effect of $CbzL_3$-VS and YU101 was only weakly pH-dependent.

Since PR39 is positively charged (theoretical pI = 12.60 according to calculation executed with ProtParam tools from the ExPASy, Swiss Institute of Bioinformatics), it is likely that the ionic interactions between the arginines of PR39 and the acidic tail of the α7 subunit (theoretical pI = 3.45) play a role in the action of the inhibitor. Figure 4 shows that the inhibitory effect of PR39 decreased with increasing pH. Although a limited range of pH accessible for titration of 20S proteasomes rendered it impossible to determine an apparent pK_a, the value of which most likely felled outside of the measurable activity of the complexes, the result strongly suggests that the ionization of charged residues, most likely arginine in PR39, is necessary for inhibition of proteasome activity. This contrasts sharply with two competitive inhibitors, $CbzL_3$-VS and YU101, upon which pH had no significant effect (Figure 4).

To define the region of PR39 involved in proteasome interaction, we generated variants of the peptide with progressive deletions starting at its COOH-terminal end. We found that the shortest peptide efficiently inhibiting the ChT-L activity of the proteasome in a dose-dependent manner consisted of 11 NH_2-terminal amino acid residues preserved from the original PR39 sequence (PR11, Figure 5). PR11 acted as a noncompetitive inhibitor and was not a substrate for the protease (data not shown).

The results collected in vitro were in perfect agreement with in vivo data. Since induction of angiogenesis by PR39 was one of the most profound in vivo effects of the peptide (*1*), we tested if shorter versions of PR peptides could promote the formation of new vessels similarly to PR39. For this purpose, we measured invasion of new blood vessels into growth factor-depleted Matrigel pellets implemented into mouse abdominal walls (*1*). Similarly to the effect of PR39, supplementing Matrigel with PR15 or PR11 induced a substantial increase of the vessel count. Peptides of shorter length were ineffective in this test (Figure 6).

To better understand the mechanism underlying PR11 activity, we sequentially mutated each residue into alanine. A single replacement with alanine did not affect the peptide's activity either in vitro or in vivo (not shown). However,

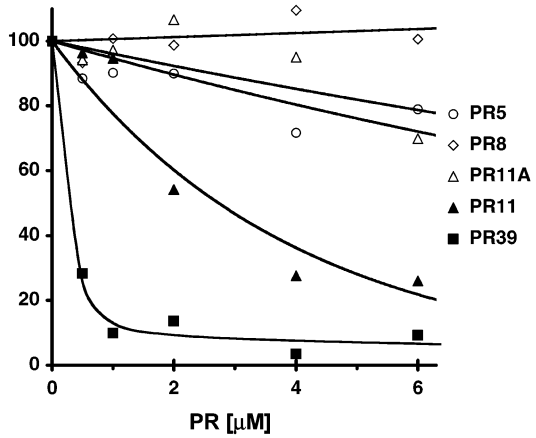

FIGURE 5: At least 11 NH_2-terminal residues containing three leading arginines are required for the inhibition of the ChT-L activity of human 20S proteasomes by the PR peptides in vitro. The dose response of ChT-L activity to increasing concentrations of the peptides was examined with SucLLVY-MCA. PR39 and PR11 almost completely inhibited proteasomes at micromolar concentrations. In comparison, the shorter peptides (PR8 and PR5) or peptides devoid of the arginines (PR11A) were very poor inhibitors of proteasomes, presumably acting as substrates and competing with the fluorogenic substrate for the active centers.

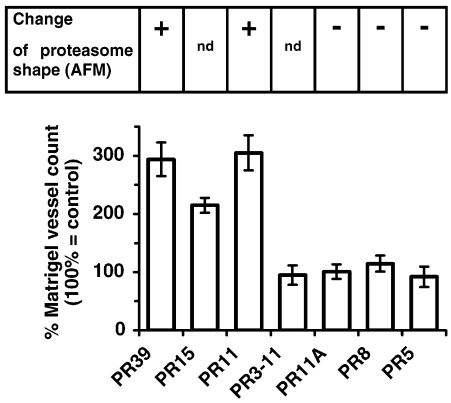

FIGURE 6: Induction of vessel growth by the PR peptides correlates with their ability to stimulate change in a shape of human 20S proteasomes. The bars show percent change of vessel count in the Matrigel plug in mice as a measure of in vivo proangiogenic activity of the PR peptides (±SD, $n = 3$), as compared with the control samples (100%) not treated with PR peptides. The strip illustrates AFM-detected changes of a shape of 20S proteasomes induced by the PR peptides (see also Figure 7). All assays were carried out with the 100 nM peptides. PR3-11 denotes a PR11 peptide with the first three NH_2 terminal residues deleted; nd, not determined.

substitution of the first three arginines of the PR11 sequence with alanines (PR11A; AAAPRPPYLPR) fully abolished PR11 activity both in vitro and in vivo (Figures 5 and 6). This observation was further supported by an examination of effect of PR11 homologues on human 20S proteasomes. Sequences of bovine (RIRPPRPRLPR), sheep, goat (both RLRPRRPRLPR), and porcine PR11 (RRRPRPPYLPR; differences underlined) are closely conserved. Indeed, these peptides also demonstrated a similar ability to inhibit in vitro ChT-L activity of 20S proteasomes (not shown). Therefore, we conclude that the essential properties of the proline and arginine-rich peptide to demonstrate its pro-angiogenic activity in an in vivo Matrigel assay and the inhibitory effect on the proteasomal peptidase activity in an in vitro assay required at least 11-residues sequence containing the NH_2-terminal arginines.

To determine global changes of the shape and dynamics of the proteasome in the presence of PR peptides, we employed atomic force microscopy (AFM). In the tapping mode AFM, a small and very sharp vibrating tip is placed in a close proximity of to the sample and interacts with the sample atoms with van der Waals forces. The topography of the sample is reflected by changes in resonant frequency or vibrational amplitude of the tip. Both the sample and the tip can be submerged in a buffer, and the method allows for relatively noninvasive imaging of native molecules in sequence. We have successfully used the method before to detect allosteric transitions in 20S proteasomes isolated from fission yeast (*14*, *15*). In our previous studies, we found that 20S proteasomes imaged with AFM had two conformations representing an open or closed entrance to the central channel. They were distinguished according to the qualitative feature of the shape of the median sections of the α rings of particles in top view orientation (Figure 7; (*14*)). Preferred conformation depended on the type of the ligand present. In a resting state or in the presence of a competitive inhibitor, the majority of the 20S proteasomes were closed most of the time. In contrast, in the presence of a substrate, the equilibrium between conformers was shifted toward the open particles. The equilibrium between conformants was stable with time, even after more that 1 hour of continuous scanning of the same field of particles. Moreover, the shift of equilibrium triggered by a substrate was fully reversible, thus strongly suggesting that the observed conformational changes were not affected by a tip contamination or gross changes in tip sharpness during repeated scanning (*15*). The presence of open and closed conformants detected by AFM is in full agreement with crystallographic data. We base this statement on two lines of evidence: (i) control eukaryotic proteasomes had a closed entrance to the central channel in crystal structure (*16*), and "closed" was the most stable conformation detected in AFM images of control 20S particles (*14*, see below); (ii) crystal structure revealed that archaebacterial proteasome from *Thermoplasma acidophilus* had always open entrance to the central channel (*17*). Consequently, AFM images of *T. acidophilus* proteasomes showed particles in open-only conformation (Gaczynska, M., and Osmulski, P. A., 2000, unpublished observations). Similarly, the mutant proteasomes with deleted gate to the central channel were open in crystal structure (*18*), and our AFM images of the mutant particles revealed only the open conformants (Gaczynska, M., and Osmulski, P. A., 2001, unpublished observations). These data strongly suggest that the open and closed conformations imaged by AFM correspond to the true physical opening and closing of the proteasomal gate, and are not a representation of nonspecific interactions of the AFM probe with a surface of the scanned protein. In the present work, we were especially interested in comparison of the effect of the noncompetitive and competitive inhibitors on dynamics of topography of proteasomes.

Human or *S. cerevisiae* 20S proteasomes were imaged as randomly oriented, cylinder-shaped particles either "standing" on their α rings (top view orientation) or "lying" on their side. As found previously for *S. pombe* 20S proteasomes (*14*, *15*), the dimensions of human and *S. cerevisiae* particles compared well to those determined on the basis of their crystal structure (*7*): 11 nm diameter and 15 nm length of the proteasomal cylinder. The top view 20S proteasomes

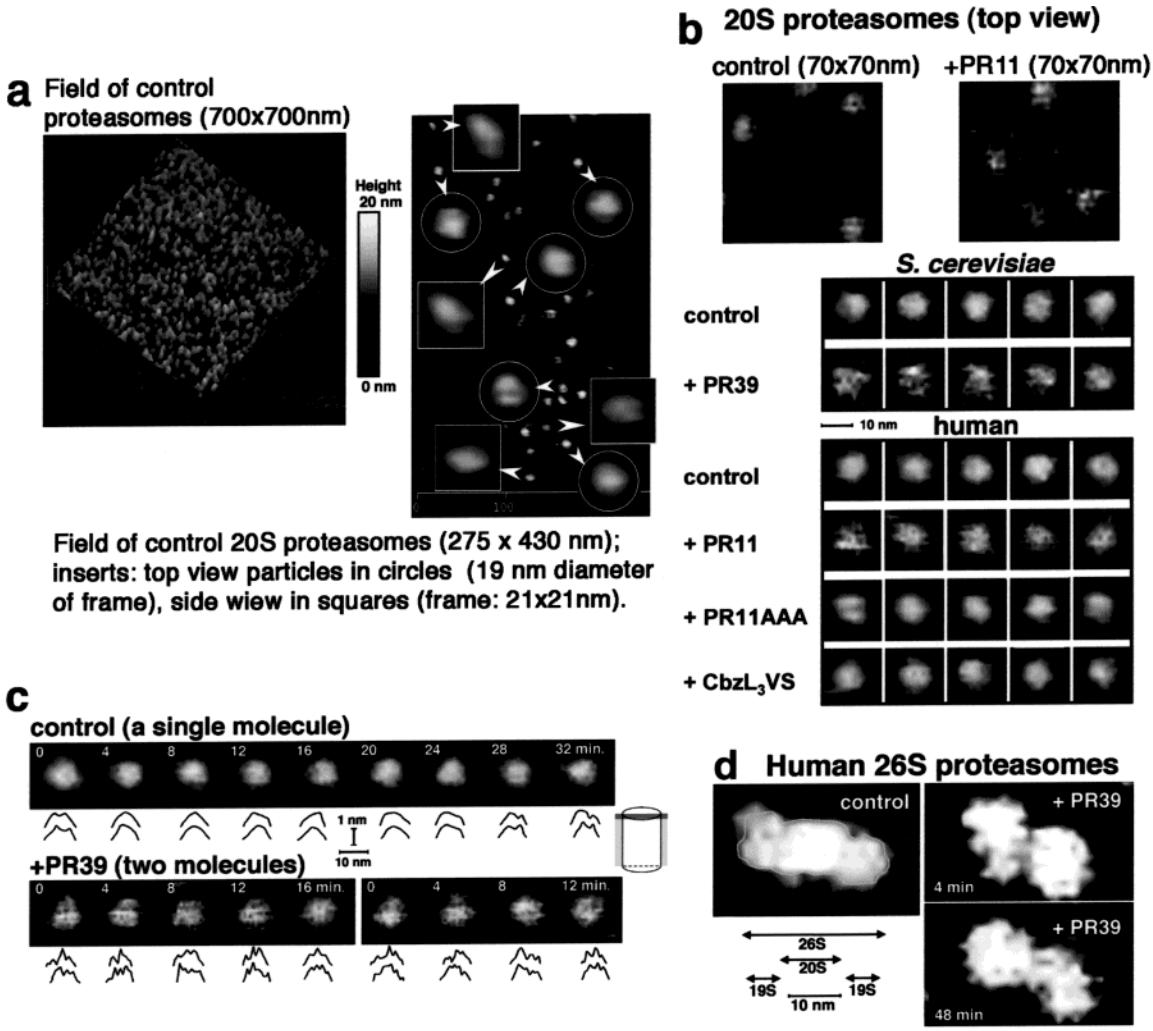

FIGURE 7: The PR peptides alter the shapes of the 20S and 26S proteasomes observed with atomic force microscopy. (a) Left: representative image of a 700 × 700 nm field of control human 20S proteasomes in the height mode. The gray-scale bar on the right side represents the height of the particles: from the baseline (black) to the highest (white). Right: representative image of a 275 × 430 nm field of control *S. cerevisiae* 20S proteasomes in the height mode with zoomed-in images of randomly selected particles in side-view and top-view orientations. (b) Top: 70 × 70 nm zoomed-in images of control human 20S proteasomes and proteasomes treated with PR11 (final concentration 5 μM). The particles in the control zoomed-in image were identified as: (clockwise from the top left) closed, a fragment of side-view particle, open, and closed. Such identification was impossible in the case of proteasomes treated with PR11 (right panel). Identical effects were observed after treatment of *S. cerevisiae*, mice, and *S. pombe* proteasomes with PR39. In the absence of proteasomes, PR peptides were not detectable with AFM. Bottom: top view images of the *S. cerevisiae* and human 20S proteasomes, control or treated with PR39 (2 μM), PR11 (5 μM), PR11A (5 μM), or a competitive inhibitor $CbzL_3$-VS (50 μM; final concentration). 20S particles were sorted into "open" and "closed" classes according to the qualitative features of median sections carried out through their α rings in four directions (*14*) . If all the sections presented a "cone", the particle was considered closed. If all the sections were "crater"-shaped, the particle was considered open. 73.4% ± 2.9% (mean ± SD; n = 35 fields with total of 762 top view molecules) of control yeast 20S proteasomes were in the closed conformation, and 73.4% ±5.3% (n = 41 fields, 1008 particles) of human 20S proteasomes were identified as closed. However, none among more than 1000 analyzed PR39-treated particles fulfilled criteria for either open or closed entrance to the central channel, as seen in (c). In contrast, 75.6% ± 3.9% (n = 25 fields, 525 particles) of human 20S proteasomes treated with PR11A were closed, and 76.3% ± 3.9% (n = 22 fields, 412 particles) of human 20S proteasomes treated with a competitive inhibitor $CbzL_3$-VS were in a closed conformation. (c) Time-lapse images of the human 20S proteasomes in the top view position. Median sections through the α rings of the molecules along vertical (top) and horizontal (bottom) axis are provided below each image. The topmost parts of about 1 nm in height of the sections are shown, as illustrated by the diagram of 20S proteasome cylinder. The dark gray part in the diagram shows the actual part of the molecule represented by the sections. The same molecules were scanned and imaged every 4 min. The control particle apparently was switching between the open (time points: 0, 28, 32 min) and closed conformations. No such changes were detected among the PR39-treated molecules, which remained in neither an open nor a closed conformation. (d) Images of a human 26S proteasome particle, control (left) and after treatment with 1 μM (final concentration) PR39 (right). After the addition of the inhibitor (4 min; upper right), the particles immediately switched to an unusual shape with seemingly enlarged 19S caps. The imaged particles remained in such conformation even after 48 min (lower right).

were easy to distinguish from side view molecules by their circular rather than oval or rectangular shape (Figure 7a). The diameter of top-view molecules measured at the half-height was 9−12 nm; however, the length of side-view proteasomes extended from 14 to 17 nm. Moreover, the top and side view particles differed in their height. The top-view human and yeast particles were 14−16 nm high, whereas the side-view particles reached only 8−11 nm.

For AFM imaging, the molecules were packed on a surface of mica, creating a loose monolayer of freely oriented top

and side view proteasomes, which were stable during repeated imaging (Figure 7a). Control proteasomes purified from all tested species showed two conformations in their top views: about 75% of the molecules were in closed (cone-shaped median section), and 25% were open (volcano shaped, Figure 7a,b). The distribution of closed and open conformants was stable with time, at least up to 2 h of continuous scanning and imaging of the same field of particles. While single particles switched conformations, they spent most of the time (about 75%) in the closed state (Figure 7c). As shown before, these conformational changes occurred with a low temporal frequency in the range of seconds, which are characteristic of allosteric motions (*14*).

After treatment with the PR peptides, proteasomes underwent striking transition in their overall shape. They appeared to stiffen and became rather motionless. When examined at higher magnification, it became apparent that the PR-treated proteasomes did not switch between the open and closed conformations (Figure 7b,c). Further evidence of a "frozen" allosteric state in PR-treated 20S proteasomes came from analysis of their median sections. Of more than 1000 inspected top view particles treated with PR39, none passed criteria established for an open or closed conformation. Instead of highly symmetrical cone shaped (closed) or concave/volcano shaped (open) median sections of control proteasomes, the treated particles were rather asymmetrical with irregular contours (Figure 7c).

In addition to human and baker's yeast, mouse and fission yeast 20S proteasomes also underwent the same structural changes when treated with PR39. The effects of PR11 on 20S proteasomes were indistinguishable from those of PR39 (Figure 7b). Importantly, 20S proteasomes treated with PR11A or a common competitive inhibitor $CbzL_3$-VS were indistinguishable from the control in their ability to switch between open and closed conformations (Figure 7b). The equilibrium between the conformers after the treatment with PR11A or with $CbzL_3$-VS remained at the level of about 75% closed and 25% open (Figure 7b). In concert with enzymatic and in vivo data, PR11A and PR8 did not affect the surface topography of 20S proteasomes (Figures 6 and 7b). Therefore, we concluded that the observed "freezing" of proteasomal conformation did not originate in force-based artifacts induced by nonspecific coating of a tip and/or a sample with the excess of the PR peptides.

The dramatic effect of PR peptides on the surface topography of 20S proteasomes was fully reversible (Figure 8). First, a field of control *S. cerevisiae* proteasomes was scanned six times every four minutes with typical distribution of the open and closed conformers. Then, 5 μM PR39 was added to the sample, and scanning resumed after 5 min (arrow A, Figure 8). At this time point, only a small population (21%) of 120 analyzed top-view proteasomes was in the definite closed (72%) or open (28%) conformation. However, it was not possible to identify conformation of the majority of particles (79%) on the basis of the median section criterion. After an additional two scans, even that small population of the regularly shaped proteasomes was not detectable, and images showed only the "frozen" particles for another eight scans. Subsequently, the inhibitor was removed from the sample with five buffer exchanges (arrow B and C in Figure 8, with estimated less than 1nM PR39 remaining), and the scanning resumed. Content of the

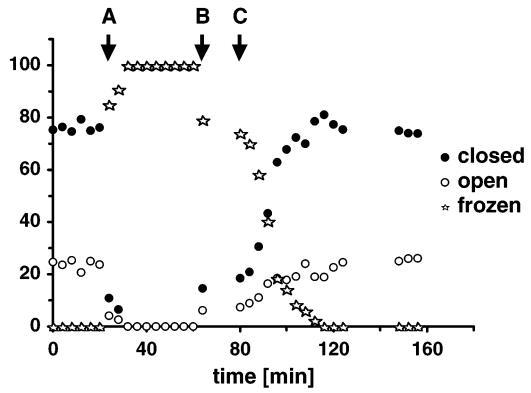

FIGURE 8: PR39-induced changes in the shape of yeast 20S proteasome observed with tapping mode AFM in liquid are fully reversible. One square micrometer AFM image was collected every 4 min. Relative content of open, closed, and "frozen" particles is shown for each time point. Between 100 and 140 molecules were analyzed for each time point. The arrows indicate when: A, PR39 was added to final concentration of 5 μM; B, the washing of the sample with a buffer without PR39 begun; C, the last wash was completed and the most of PR39 was removed from the sample. The treated 20S proteasomes relaxed slowly after removal of the inhibitor in contrast with their fast freezing upon the addition of PR39. During the relaxation period, a fraction of open particles was observed in excess compared to the resting state.

"frozen" proteasomes decreased with each scan; however, their complete elimination took up to 10 scans. The slow relaxation accompanied by a relative excess of open particles suggests that PR39 is a tightly binding inhibitor. Additionally, it indicates that the relaxation process leading to the distribution of the conformers specific for the resting state proceeds initially via open particles. Unfortunately, this observation could not be confirmed by the enzymatic studies since the complete removal of PR39 from the sample with the centrifugal concentrator required a similar time span as the AFM-detected relaxation.

A field of purified human 26S proteasomes was observed under the same conditions as those used for imaging the 20S particles. In this case, only side view molecules could be observed. The 26S complexes were typically found with one or two dragonhead-shaped 19S caps attached to the 20S core. After the treatment with PR39, we noticed a dramatic transition in the shape of the molecules. They immediately lost features typical of the 26S complexes, giving the impression that two 19S caps almost touched each other with hardly recognizable 20S core. In addition to being grossly misshaped, they also did not show any obvious dynamics (Figure 7d). Although at this point in our studies, we cannot explain these observations in detail, we speculate that either the 19S caps partially dissociated or they vibrated too fast for recognition of 20S core. These findings fully correlate with the inhibition of 26S proteasome by PR39. Moreover, they also agree with the observed interference of PR39 with the reassembly of 26S proteasomes from 20S and 19S particles (Figure 3).

In conclusion, the data in this study show that PR peptides as short as 11 residues, with three NH_2-terminal arginines exhibit a potential to interfere with the conformation of both 20S and 26S proteasomes leading to the inability of the enzyme to switch between the open and closed conformations in vitro. Collectively, the changes trigger a strong but reversible inhibition of the peptidase activities of proteasome.

Since the PR peptides act as noncompetitive inhibitors simultaneously affecting the specific peptidase activities to a different degree, we speculate that PR39 does not plug the entrance to the proteasome but instead it exercises its influence through interactions with a rim of the α ring. Importantly, the observed in vitro inhibitory and conformational effects fully correlate with the ability of the peptides to promote angiogenesis in vivo.

Although the molecular mechanism through which the PR peptides achieve their unusual inhibitory specificity in vivo remains unclear, it seems indisputable that they show an enormous potential as antiinflammatory agents and regulators of angiogenesis. We plan to pursue aggressively these issues first addressing molecular events directing specific binding of the PR peptides to the proteasomes and how that binding translates into inhibition of the giant protease.

REFERENCES

1. Li, J., Post, M., Volk, R., Gao, Y., Li, M., Metais, C., Sato, K., Tsai, J., Aird, W., Rosenberg, R. D., Hampton, T. G., Sellke, F., Carmeliet, P., and Simons, M. (2000) *Nat. Med. 6*, 49−55.
2. Bao, J., Sato, K., Li, M., Gao, Y., Abid, R., Aird, W., Simons, M., and Post, M. J. (2001) *Am. J. Physiol. Heart Circ. Physiol. 281*, H2612−H2618.
3. Hoffmeyer, M. R., Scalia, R., Ross, C. R., Jones, S. P., and Lefer, D. J. (2000) *Am. J. Physiol. Heart Circ. Physiol. 279*, H2824−H2828.
4. Ikeda, Y., Young, L. H., Scalia, R., Ross, C. R., and Lefer, A. M. (2001) *Cardiovasc. Res. 49*, 69−77.
5. Korthuis, R. J., Gute, D. C., Blecha, F., and Ross, C. R. (1999) *Am. J. Physiol. 277*, H1007−H1013.
6. Gao, Y. H., Lecker, S., Post, M. J., Hietaranta, A. J., Li, J., Volk, R., Li, M., Sato, K., Saluja, A. K., Steer, M. L., Goldberg, A. L., and Simons, M. (2000) *J. Clin. Invest. 106*, 439−448.
7. Voges, D., Zwickl, P., and Baumeister, W. (1999) *Annu. Rev. Biochem. 68*, 1015−68.
8. Zwickl, P. (2002) *Curr. Topics Microbiol. Immunol. 268*, 23−41.
9. Adams, J. (2002) *Oncologist 7*, 9−16.
10. Almond, J. B., and Cohen, G. M. (2002) *Leukemia 16*, 433−443.
11. Myung, J., Kim, K. B., and Crews, C. M. (2001) *Med. Res. Rev. 21*, 245−273.
12. Driscoll, J., and Goldberg, A. L. (1990) *J. Biol. Chem. 265*, 4789−4792.
13. Gaczynska, M., Rock, K. L., and Goldberg, A. L. (1993) *Nature 365*, 264−267.
14. Osmulski, P. A., and Gaczynska, M. (2000) *J. Biol. Chem. 275*, 13171−13174.
15. Osmulski, P. A., and Gaczynska, M. (2002) *Biochemistry 41*, 7047−7053.
16. Groll, M., Ditzel, L., Lowe, J., Stock, D., Bochtler, M., Bartunik, H. D., and Huber, R. (1997) *Nature 386*, 463−471.
17. Lowe, J., Stock, D., Jap, B., Zwickl, P., Baumeister, W., and Huber, R. (1995) *Science 268*, 533−539.
18. Groll, M., Bajorek, M., Kohler, A., Moroder, L., Rubin, D. M., Huber. R., Glickman, M. H., and Finley, D. (2000) *Nat. Struct. Biol. 7*, 1062−1067.

BI034784F